Goswami P. et al., 2016

Volume 2 Issue 3, pp. 40 - 54

Date of Publication: 15th November, 2016

DOI- https://dx.doi.org/10.20319/Mijst.2016.23.4054

This paper can be cited as: Goswami, P., Mandal, D. K., Manna, N. K., & Chakrabarty, S., (2016). Analysis of Wall Shear Parameters of Physiological Pulsatile Flow through Mild and Severe Arterial Stenosis and Correlation to Atherosclerosis. Matter: International Journal of Science and Technology, 2(3), 40-54.

ANALYSIS OF WALL SHEAR PARAMETERS OF PHYSIOLOGICAL PULSATILE FLOW THROUGH MILD AND SEVERE ARTERIAL STENOSIS AND CORRELATION TO ATHEROSCLEROSIS

Partha Goswami
Mechanical Engineering Department, Jadavpur University, Kolkata, India
gospartha@gmail.com

Dipak Kumar Mandal
Mechanical Engineering Department, College of Engineering & Management, Kolaghat, Midnapur(E), India
dipkuma@yahoo.com

Nirmal Kumar Manna
Mechanical Engineering Department, Jadavpur University, Kolkata, India
nkmanna@mech.jdvu.ac.in

Somnath Chakrabarty
Mechanical Engineering Department, Indian Institute of Engineering, Science and Technology, Shibpur, Howrah, India
somnathbec@rediffmail.com

Abstract

Numerical simulations of physiological pulsatile flow through mild and severe arterial stenosis are carried out to analyze wall shear stress parameters. The governing equations are solved by finite volume method. The study shows that the distribution patterns of time-averaged wall shear stress (TAWSS), oscillatory shear index (OSI) and relative residence time (RRT) are same for both mild stenosis and severe stenosis. The magnitude of peak TAWSS and low TAWSS and extent of negative TAWSS of severe stenosis is higher than those of mild stenosis. The OSI value of severe stenosis is higher at distal to throat of stenosis in comparison to mild stenosis. The size of recirculation zone of severe stenosis is larger than that of mild stenosis. The abnormally high peak value of RRT of severe stenosis is concentrated and located at far away from stenosis when it is compared with mild stenosis.

Keywords

Atherosclerosis, Oscillatory shear index, Pulsatile, Relative residence time, Wall shear stress

1. Introduction

Atherosclerosis, a cardiovascular disease, is a process of narrowing and hardening of arterial wall by depositing of lipid streaks in the inner wall of an artery. The arterial stenosis is the segment of artery which is narrowed, restricted and hardened. Thus stenosis obstructs flow of blood through artery and this obstruction changes the flow dynamics of blood flow, which have a pathological significance and correlation to atherosclerosis and other cardiovascular disease. Many researchers have investigated pulsatile blood flow through stenosis because of the importance of hemodynamic parameters, particularly wall shear parameters in the development of arterials diseases. The distribution of wall shear stress (WSS) and the localization of disease, atherosclerosis, is the main interest of investigation in arterial flow studies. Gay and Zhang, 2008 have numerically studied the blood flow through stenosed artery and investigated WSS, oscillatory shear index (OSI) and relative residence time (RRT). Lee, Antiga & Steinman, 2009 have recommended the use of RRT as a strong parameter of low and oscillatory shear flow. Kinght et al., 2010 have done patient specific computation study on the wall shear parameters. They suggested time averaged wall shear stress (TAWSS), OSI and RRT are the important

factors to predict the areas of plaque formation. Ryou, Kim, Kim & Cho, 2012 have analyzed and compared the flow characteristics of the healthy vessel and diseased vessel through computational fluid dynamics simulation and concluded that low TAWSS and high OSI are widely accepted indicators of plaque formation or the direction of plaque progression. Peiffer, Sherwin & Weinberg, 2013 have reviewed the oscillating shear stress along with low magnitude of WSS in relation to the initiation and development of atherosclerosis. They stated that low and oscillating shear theory is less robust than commonly assumed. Liu, 2013 has done the patient specific coronary arterial blood flow simulation to investigate the distribution pattern of the wall shear stress on the inner surface of artery. From the literature reviews, this can be assumed that the progression of atherosclerosis depends on hemodynamic features, especially WSS, OSI and RRT. But a large number of further studies on these hemodynamic parameters are still necessary in different ways for accurate and feasible understanding the relation between blood flow and atherosclerosis, and this information of will be useful tool of diagnosis tool of the disease, atherosclerosis. Therefore, a numerical simulation based on finite volume method is carried out on physiological pulsatile flow through artery with mild stenosis and severe stenosis and the wall shear parameters are calculated from simulated results are investigated in order to improve our understanding. In this work, the rigid arterial wall has been considered. The elasticity of wall of artery is reduced as the arteriosclerosis is developed in the artery [Liu, Wang, Ai & Liu, 2004]. It is assumed that the stenosis depends on axial distance and height of its growth. In our work, the bell shaped stenosis is considered and the developed stenosis in the arterial wall is axially non-symmetric and radially symmetric. The blood, flow through the artery, is considered as Newtonian fluid and incompressible, and flow as physiological pulsatile flow.

2. Problem Formulation

The dimensionless diameter and length of model artery are taken as 1 and 200 respectively. The length between the throat of stenosis and the entry is 50. The flow geometry of stenosed artery and the stenosis models are illustrated in Fig.1a and Fig.1b. This stenosis is considered as bell-shaped and the geometry of the stenosis is drawn mathematically from the following equation [Misra & Shit, 2006]

$$r = 0.5 - h_f \exp\left(-\frac{4m^2 z^2}{L_s{}^2}\right) \qquad \ldots\ldots (1)$$

Where, m is a parametric constant.

In clinical medicine, degree of stenosis, percentage stenosis or percentage of restriction is defined as follows [Wootton & Ku, 1999]:

$$PR = \frac{D-(D-h_f)}{D} \times 100\% \qquad \ldots\ldots (2)$$

In our work, PR 30% and PR 70% are considered as mild stenosis and severe stenosis respectively. The dimensions of stenosis model with varying percentage of restriction are shown in Fig.1b.

It is assumed that the flow is axisymmetric and two dimensional. The fluid is incompressible and Newtonian with constant fluid properties. The differential conservation forms of the both of continuity and Navier-Stokes equations in cylindrical co-ordinates (r,z) have been given below:

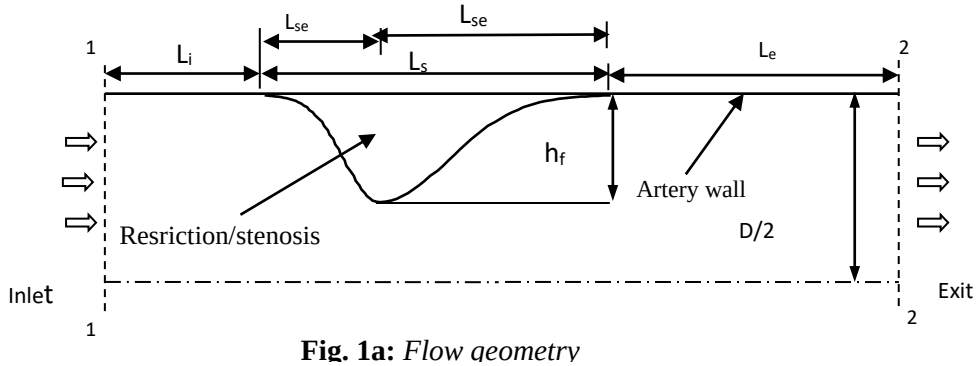

Fig. 1a: *Flow geometry*

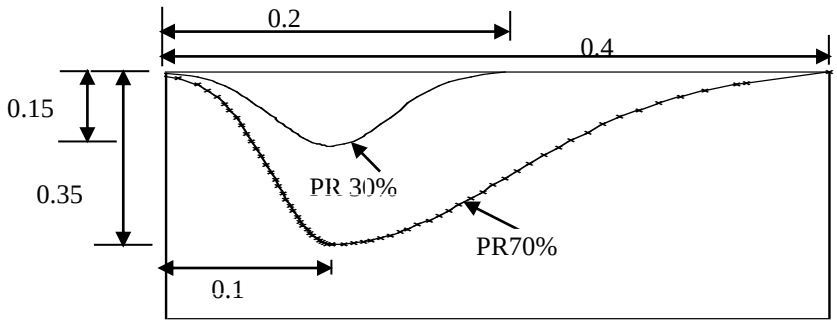

Fig. 1b: *Stenosis model*

Continuity equation:

$$\frac{1}{r}\frac{\partial(ru_r)}{\partial r}+\frac{\partial u_z}{\partial z}=0 \qquad \ldots\ldots (3)$$

r-direction momentum equation:

$$\frac{\partial u_r}{\partial t}+u_r\frac{\partial u_r}{\partial r}+u_z\frac{\partial u_r}{\partial z}=-\frac{1}{\rho}\frac{\partial p}{\partial r}+\frac{\mu}{\rho}\left[\frac{\partial}{\partial r}\left(\frac{1}{r}\frac{\partial(ru_r)}{\partial r}+\frac{\partial^2 u_r}{\partial z^2}\right)\right] \qquad \ldots\ldots. (4)$$

z-direction momentum equation:

$$\frac{\partial u_z}{\partial t}+u_r\frac{\partial u_z}{\partial r}+u_z\frac{\partial u_z}{\partial z}=-\frac{1}{\rho}\frac{\partial p}{\partial z}+\frac{\mu}{\rho}\left[\frac{\partial}{\partial r}\left(\frac{1}{r}\frac{\partial(ru_z)}{\partial r}+\frac{\partial^2 u_z}{\partial z^2}\right)\right] \qquad \ldots\ldots. (5)$$

The dimensionless variables of lengths, time, velocities and pressure are as follows:

$r^* = r/D$, $z^* = z/D$, $L^* = L/D$, $t^* = t/T$. $u_r^* = u_r/U$, $u_z^* = u_z/U$ and $p^* = p/\rho U^2$.

The above governing equations are non-dimensionalized and the equations are given below:

$$\frac{1}{r^*}\frac{\partial(r^* u^*_r)}{\partial r^*}+\frac{\partial u^*_z}{\partial z^*}=0 \qquad \ldots\ldots (6)$$

$$\frac{1}{\pi}\frac{W_o^{\,2}}{R_e}\frac{\partial u^*_r}{\partial t^*}+u^*_r\frac{\partial u^*_r}{\partial r^*}+u^*_z\frac{\partial u^*_r}{\partial z^*}=-\frac{\partial p^*}{\partial r^*}+\frac{2}{R_e}\left[\frac{\partial^2 u^*_r}{\partial r^{*2}}+\frac{\partial^2 u^*_r}{\partial z^{*2}}+\frac{1}{r}\frac{\partial u^*_r}{\partial r^*}\right] \qquad \ldots.. (7)$$

$$\frac{1}{\pi}\frac{W_o^{\,2}}{R_e}\frac{\partial u^*_z}{\partial t^*}+u^*_r\frac{\partial u^*_z}{\partial r^*}+u^*_z\frac{\partial u^*_z}{\partial z^*}=-\frac{\partial p^*}{\partial r^*}+\frac{2}{R_e}\left[\frac{\partial^2 u^*_z}{\partial r^{*2}}+\frac{\partial^2 u^*_z}{\partial z^{*2}}+\frac{1}{r}\frac{\partial u^*_z}{\partial r^*}-\frac{u^*_z}{r^{*2}}\right] \qquad \ldots.. (8)$$

Where Wo is the Womersley number and Re is the Reynolds number.

The Womersley number is stated as

$$W_o = R\sqrt{\frac{\omega}{\nu}} \qquad \ldots\ldots (9)$$

Where ω is the radial frequency ($2\pi / \mathrm{T}$) of the flow. The Womersley number is defined as the ratio of unsteady force to viscous force. The Womersley number indicates the frequency of the pulsatile flow. The Womersley number has been assumed as 10 in this study.

Re is the Reynolds number, which is defined as

$$R_e = \frac{\rho UD}{\mu} \quad \ldots\ldots (10)$$

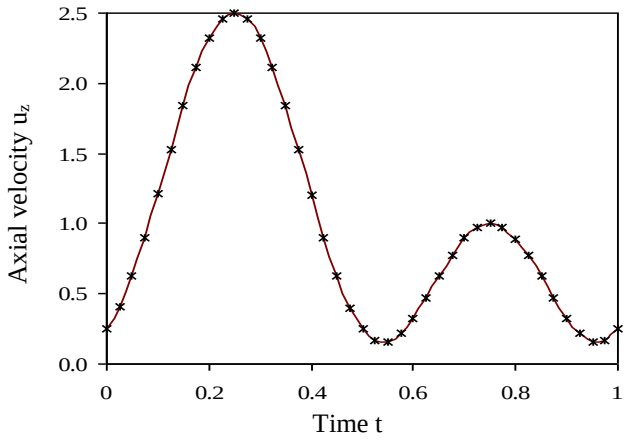

Fig. 2: *Waveform of physiological pulsatile flow*

The Reynolds number is defined as the ratio of inertia force to viscous force. The Reynolds number has been assumed as 100 in this study.

The boundary conditions have been applied to solve the governing equations. The blood flow has no slip condition at the wall, i.e., $u_r^* = 0$, $u_z^* = 0$. The flow is fully developed and physiological pulsatile flow in axial direction at the inlet of the modeled flow domain, i.e., $u_z^* = 1 + 0.75\sin\omega t^* - 0.75\cos 2\omega t^*$. There is no velocity in radial direction, i.e., $u_r^* = 0$ at inlet, exit and the line of symmetry. The fully developed flow condition has been considered at the exit of the domain and thereby the velocity gradient is zero, i.e., $\partial u_z^* / \partial x^* = 0$, The normal gradient of the axial velocity at the line of symmetry is assumed to be zero, i.e., $\partial u_r^* / \partial z^* = 0$.

3. Results

The numerical results obtained from the simulation using the in-house CFD code [Goswami, Mandal, Manna and Chakrabarty, 2014] are compared with the numerical and experimental results of Womerseley, 1955 and Ojha, Cobbold, Johnston & Hummel, 1989 respectively. The results of CFD simulations are found to be a good agreement the results of the experiment, which is shown by Goswami et al., 2014. The TAWSS, OSI and RRT have been taken into consideration for the analyzing of hemodynamic features of physiological pulsatile flow through the stenosed arteries with mild stenosis and severe stenosis.

The wall shear stresses, obtained from the simulation results at different time levels, are averaged over one cardiac cycle for better understanding of peak and low WSS. The TAWSS can be obtained by integrating of all instantaneous wall shear stress over a cardiac cycle.

$$\text{TAWSS}=\overline{\tau_w^*}=\frac{1}{T}\int_0^T \tau_w dt \qquad \ldots\ldots (11)$$

Blood flow velocity changes in the restriction zone and wall shear changes drastically as well. Therefore, it is very imperative to observe the distribution pattern of wall shear stress in the

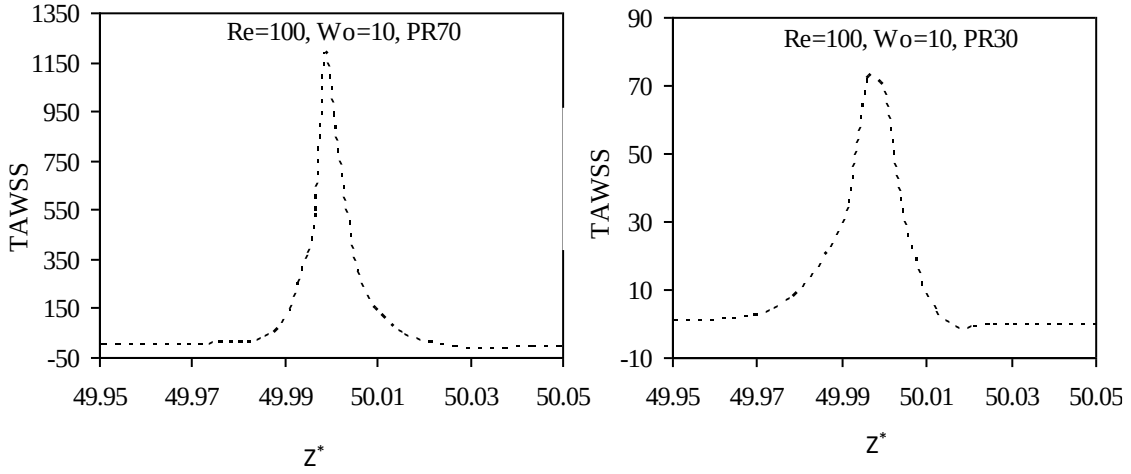

Fig. 3: *Distribution pattern of time averaged peak wall shear stress at stenotic zone for PR30 and PR 70*

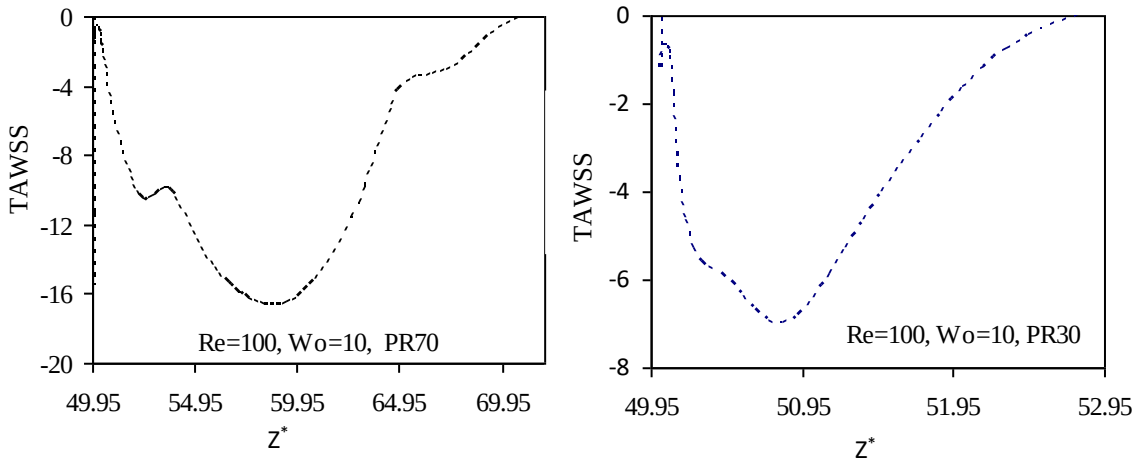

Fig. 4: *Distribution pattern of time averaged low wall shear stress at post-stenotic zone for PR30 and PR70*

stenotic zone. The distribution pattern of the TAWSS along axial direction of arterial length in the stenosis zone is depicted in Fig.3 for both mild stenosis and severe stenosis. It is revealed that the nature of variation of the time-averaged WSS is almost similar for mild and severe stenosis. As the flow area is lowered at the throat of the stenosis, the velocity gradient is maximum at this location. TAWSS is increased sharply just when the flow reaches to the throat of the stenosis and again the TAWSS is decreased sharply just when the blood flow exits from the throat as shown in figure. This is also observed from the figure that the magnitude of peak WSS is very high for severe stenosis in comparison to mild stenosis. The high shear stress harms the artery wall mechanically and thereby promotes the diseases, atherosclerosis [Fry, 1968]. These high levels of TAWSS cause direct endothelial damage by platelets activation and increase the risk of clotting the blood flow [Malek, Alper & Izumo, 1999]. This condition is very probable in atherosclerosis disease and basically the main cause of heart attacks [Razavi, Shirani & Sadeghi, 2011]. The Fig.4 displays the distribution pattern of low TAWSS at the post-stenotic zone along axial direction of arterial length for both mild and severe stenosis separately. When the blood flow leaves the throat of the stenosis, the velocity gradient is lowered. WSS changes the direction from the positive to negative at the downstream flow. The adverse pressure gradient creates and a flow separation is formed just after the stenosis. The figure of low WSS depicts that the magnitudes of maximum low wall shear stress and area for the low wall shear stress zone for

severe stenosis are higher than those of mild stenosis. Low mass diffusion of lipids is occurred in the region of low WSS and thus atherosclerosis is loaclized [Caro, Fitz-Gerald & Schroter, 1971]. From the figure it is also observed that the TAWSS reaches at zero value two times for both of mild stenosis and severe stenosis. The velocity gradient is zero means the magnitude of TAWSS is zero. Both of the separation and stagnation points of the blood flow are the stagnation points which are the points of zero velocity gradients.

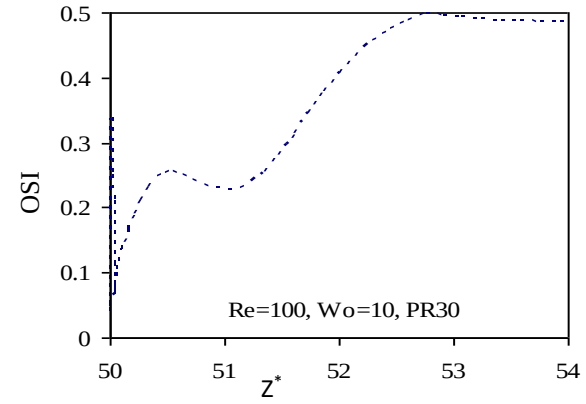

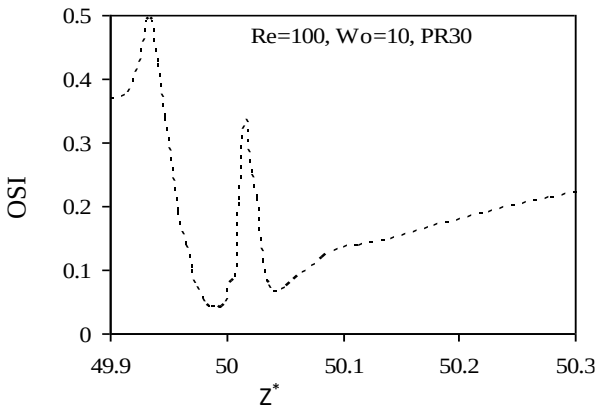

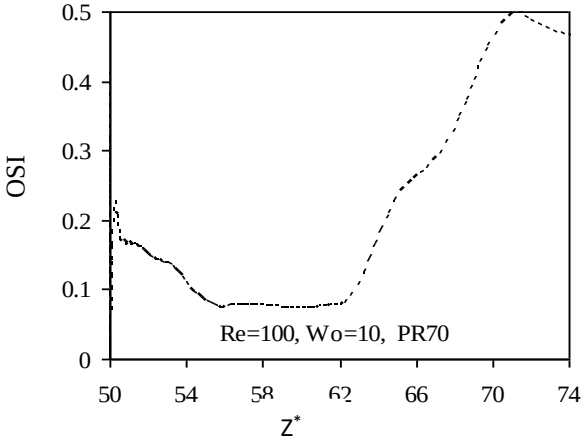

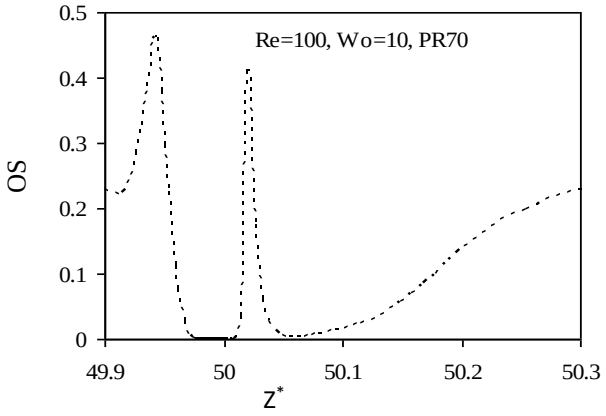

Fig. 5: *Variation of Oscillatory Shear Index at Post-stenotic Zone for PR30 and PR70*

Fig 6: *Variation of oscillatory Shear Index at stenotic zone for PR30 and PR70*

Oscillatory Shear Index (OSI) is a derivative of wall shear stress. OSI defines the cyclic departure of the WSS vector from its major axial direction [Ku, Giddens, Zarins & Glagoy, 1985, He &Ku, 1996]. The OSI is calculated from the following formula:

$$OSI = \frac{1}{2}\left[1 - \frac{\left|\int_0^T \tau_w dt\right|}{\int_0^T |\tau_w| dt}\right] \qquad \ldots\ldots (12)$$

From the above formula, it is clearly estimated that the maximum value of OSI is 0.5 and the minimum vale is 0. When the instantaneous WSS is aligned with the TAWSS throughout the cardiac cycle, the OSI becomes zero. When the instantaneous WSS does not align with the TAWSS, the OSI becomes 0.5. Thus high OSI value indicates the region of disturbed flow. The calculated OSI values at stenotic zone for both mild and severe stenosis are shown in Fig.6. Sharp increase and decrease in OSI value are observed at just immediate of throat of stenosis. This peak OSI point indicates the point of flow separation. The calculated OSI values at post-stenotic zone for both mild and severe stenosis are shown in Fig.5 and Fig.6. The OSI patterns are very similar for the two cases, mild stenosis and severe stenosis. After the flow separation, the OSI value maintains at low levels up to a certain point along axial distance, where the OSI value suddenly reaches the maximum value. This point indicates the point of flow reattachment. The vortex is formed near the arterial stenosis as shown in Fig. 7 and Fig8, which causes the OSI to increase and decrease locally at stenotic and post-stenotic zone. The OSI value of severe stenosis is higher at just after the throat of the stenosis than the same of severe stenosis. The size of the recirculation zone is larger in case of severe stenosis. This is also justified from the figure of the distribution pattern of low WSS.

Relative residence time (RRT) describes that how long time a particle resides at a particular location. Himburg et al., 2006 showed that the residence time of particles near the wall is proportional to a combination of averaged wall shear stress (AWSS) and OSI.

$$RRT \propto \frac{1}{(1 - 2.OSI)AWSS} \qquad \ldots. (13)$$

Where,

$$AWSS = \frac{1}{T}\int_0^T |\tau_w| dt \qquad \ldots. (14)$$

From the equation it is cleared that RRT will be high when OSI value increases and averaged wall shear stress decreases. The relative residence time of both mild and severe stenosis are shown in Fig.9. The magnitude of peak RRT for severe stenosis is significantly higher than the same for mild stenosis. The peak relative residence time is located far away from the throat of stenosis in case of severe stenosis in comparison to mils stenosis as shown in Fig.9 and this result is same as the results obtained by Gay and Zhang, 2008. This peak RRT locates the regions with high OSI and low WSS. This low averaged shear stress and high OSI may be significant condition in the development and localization of atherosclerotic plaque in the inner wall of artery as suggested by Ku et al., 1985.

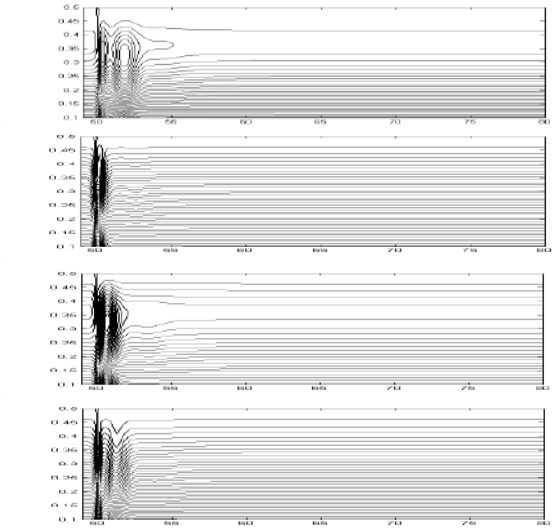

Fig. 7: *Stream line contours for 30% restriction for time steps 0, 0.25, 0.5 and 0.75 (from top to bottom)*

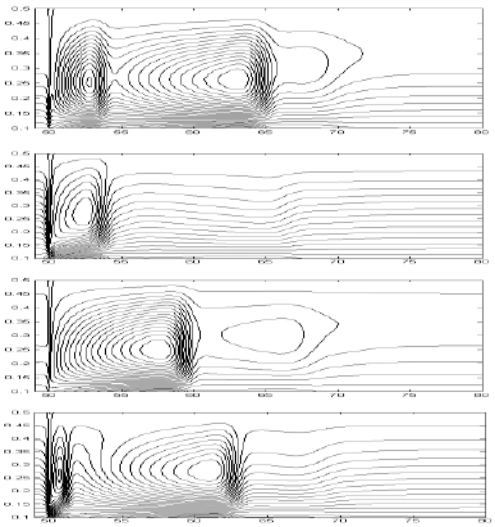

Fig. 8: *Stream line contours for 70% restriction for time Steps 0, 0.25, 0.5 and 0.75 (from top to bottom)*

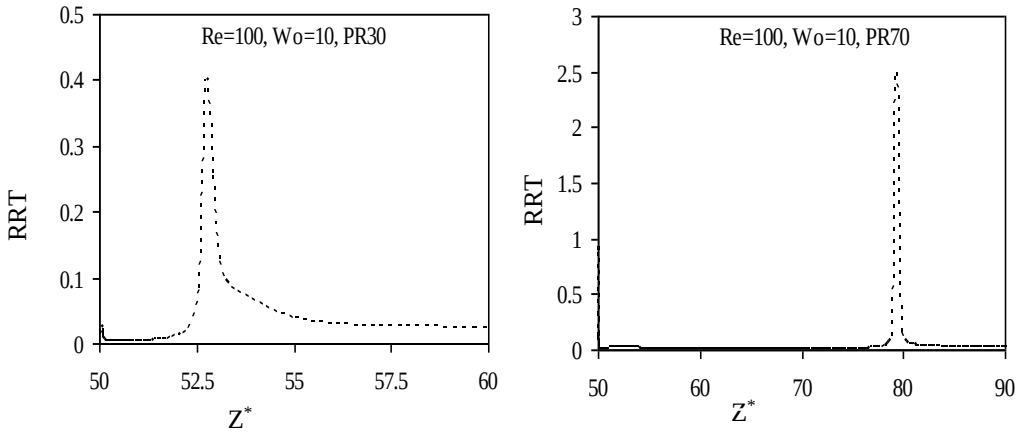

Fig. 9: *Variation of relative residence time along axial direction at post-stenotic zone for PR30 and PR70*

4. Conclusions

In this work, it is observed that high wall shear stresses are limited to the area near the throat of the stenosis for both the case of mild stenosis and severe stenosis, and the magnitude is very high for severe stenosis. This high shear stress activates platelets and thus induces thrombosis, a cardio vascular disease. Thrombosis fully restricts blood flow to the heart or brain through artery [Ku, 1997]. The time-averaged low wall shear stress of severe stenosis is higher than that of mild stenosis and the size of recirculation zone of severe stenosis is lager than that of mild stenosis, which is justified by low TAWSS and OSI results. These regions with low shear stress and flow recirculation are susceptible to fatty deposition [Caro, 2009]. The peak RRT, emerges as an appropriate tool for identifying the possible regions of atherosclerotic plaque localization [Himburg et al., 2004], is localized at far away from the stenosis with higher value in case of severe stenosis. Though the chances of atherosclerosis are dominated for both of the cases, the severe stenosis is susceptible to the atherosclerosis along with other vascular disease.

5. Appendix

D Dia of the artery, [m]

L Total length of computational domain, [m]

T Time period of the pulsatile cycle, [s]

R Radius of artery, [m]

L_s Length of stenosis, [m]

u_z Velocity in z-direction, [ms^{-1}]

u_r Velocity in r-direction, [ms^{-1}]

U Average velocity in r-direction at inlet, [ms^{-1}]

r, z Cylindrical co-ordinates

L_{is} Length of upstream stenosis, [m]

L_{es} Length of downstream stenosis, [m]

L_s Total length of computational domain up to stenosis, [m]

L_e Total length of computational domain after stenosis, [m]

μ Dynamic viscosity, [kg $m^{-1}s^{-1}$]

ρ Density, [kg m^{-3}]

p Static pressure, [Nm^{-2}]

t Time, [s]

υ Kinematic viscosity, [ms^{-2}]

References

Caro, C. G.(2009). Discovery of the role of wall shear in atherosclerosis, 2009, Arterioscler Thromb Vasc Biol, 29, 158-162.

Caro, C.G., Fitz-Gerald, J. M., & Schroter, R. C. (1971). Atheroma and arterial wall shear: observation, correlation and proposal of a shear dependent mass transfer mechanism for atherogenesis, Proc. R. Soc. Lond. B. Biol. Sci, 17(7), 109-159.

Fry, D. L. (1968). Acute vascular endothelial changes associated with increased blood velocity gradients, Circ. Res., 12, 165-197.

Gay, M., & Zhang, L. T. (2008). Numerical studies of blood flow in healthy, stenosed, and stented carotid arteries, Int. J. Numer. Meth. Fluids, DOI: 10.1002/fld1966.

Goswami, P., Mandal, D. K., Manna, N. K., & Chakrabarty, S. (2014). Study on the effect of steady, simple pulsatile and physiological pulsatileflows through a stenosed artery, Heat Mass Transfer, 50, 1343-1352.

He, X., & Ku, D. N. (1996). Pulsatile Flow in the Human Left Coronary Artery Bifurcation: Average Conditions, Journal of Biomechanical Engineering, 118, 74-82.

Himburg, H. A., Grzybowski, D. M., Hazel, A. L., Lamack, A, J. A., Li, X. M., & Friedman, M. H. (2004). Spatial Comparison between Wall Shear Stress Measures and Porcine Arterial Endothelial Permeability, American Journal of Physiology - Heart and Circulatory Physiology, 286, 1916-1922.

Kinght, J., Olgac, U., Saur, S. C., Poulikakos, D. W., Cattin, P. C., Kurtcuoglu, H. V. (2010). Choosing the optimal wall shear parameter for the prediction of plaque location—A patient-specific computational study in human right coronary arteries, Atherosclerosis, 211, 445-450.

Ku, D. N. (1997). Blood flow in arteries, Annu. Rev. Fluid Mech., 29, 399–434.

Ku, D. N., Giddens, D. P., Zarins, C. K., & Glagoy, S. (1985) Pulsatile flow and atherosclerosis in the human carotid bifurcation—positive correlation between plaque location and low and oscillating shear– stress, Arteriosclerosis, 5, 293–302.

Liu, B. (2013). The Wall Shear Stress of a Pulsatile Blood Flow in a Patient Specific Stenotic Right Coronary Artery, Engineering, 5, 396-399.

Liu, G.T., Wang, X. J., Ai, B. Q., & Liu, L. G. (2004) Numerical Study of Pulsating Flow Through a Tapered Artery with Stenosis, Chinese Journal of Physics , 42(4-1), 401-409.

Lee, S. W., Antiga, L., & Steinman, D. A. (2009). Correlations among indicators of disturbed flow at the normal carotid bifurcation, Journal of Biomechanical Engineering, 131, 061013 (1-7).

Malek, A. M., Alper, S. L., & Izumo, S. (1999). Hemodynamic shear stress and its role in atherosclerosis, JAMA, 282, 2035-2042.

Misra, J. C., & Shit, G. C. (2006). Blood Flow Through arteries in a Pathological State: A Theoretical study, International Journal of Engineering Science, 44, 662-671.

Ojha, M., Cobbold, R.S.C., Johnston, K.W., & Hummel, R.L. (1989) Pulsatile flow through constricted tube: an experimental investigation using photochromic tracer method, Journal of Fluid Mechanics, 203, 173–197.

Patankar, S.V. (1980) Numerical Heat Transfer, North Holland.

Peiffer, V., Sherwin, S. J., & Weinberg, P. D. (2013). Does low and oscillatory wall shear stress correlate spatially with early atherosclerosis? A systematic review, Cardiovascular Research , 99, 242–250.

Razavi, A., Shirani, E., & Sadeghi, M. R. (2011). Numerical simulation of blood pulsatile flow in a stenosed carotid artery using different rheological models, Journal of Biomechanics, 44, 2021–2030.

Ryou, H. S., Kim, S., Kim, S.W., & Cho, S. W. (2012) Construction of healthy arteries using computed tomography and virtual histology intravascular ultrasound, Journal of Biomechanics, 45, 1612–1618.

Sherwin, S. J., & Blackburn, H. M. (2005). Three-dimensional instabilities and transition of steady and pulsatile axisymmetric stenotic flows, J. Fluid Mech., 533, 297–327.

Womersley, J. R. (1955). Method for the calculation of velocity, rate of flow, and viscous drag in arteries when the pressure gradient is known, J. Physiol, 127, 553-563.

Wootton, D. M., & Ku, D. N. (1999). Fluid mechanics of vascular systems, diseases, and thrombosis, Annual Review of Biomedical Engineering, 1, 299–329.